



## T.1: All Solid State Pulsed Power Supply for Copper Vapour Lasers

*D. V. Ghodke (dvghodke@rrcat.gov.in) and  
K. Muralikrishnan.*

### 1. Introduction:

The copper vapour laser (CVL) is a high repetition rate, longitudinal discharge laser with an optical output in both green and yellow wavelengths at 510.6 nm and 578.2 nm respectively. Population inversion is created in the metal vapour by means of electrical discharge. As the population inversion lasts for a very short time, the discharge has to be essentially pulsed. In most of the CVLs, the electrical discharge is provided using a capacitor-to-capacitor charging circuit giving an electrical pulse with a rise time of less than 100 ns, voltage amplitude of -15 kV and peak pulse current of about 800 A. To achieve these specifications, conventional pulsed power supply circuits use thyatron as the main switching device to produce pulses in capacitor to capacitor charging circuits. These lasers are self-heated by discharge. The energy required for heating and vaporizing copper is supplied by the discharge itself. It operates at a repetition rate of 5 to 7 kHz. The major drawback of the thyatron based pulsed discharge circuit is limited lifetime (<1000 hrs.) of the switching device (Thyatron). This increases the operational cost of the pulse power supply, as the switching device needs to be replaced after a pre-determined time. The lifetime of a thyatron depends on the peak anode current, the repetition rate, the rate of rise of anode current, the plate break down voltage, and the anode-heating factor. There are reports [1] on improvement of life time of the thyatron by reducing the peak anode current and rate of rise of anode current by introducing a magnetic assist and magnetic pulse compression (MPC) technique. However, such circuits did not gain much popularity due to the unavoidable use of the thyatron. On the contrary, single solid-state devices generally do not have the peak voltage and current rating required for such applications and consequently, many devices are usually required for their use in fast high voltage circuits. In recent years, pulse power supplies based on solid-state switches with MPC have gained popularity due to very high lifetime. The switches used in the earlier development circuits were based on thyristor family devices. Later, these switching devices were replaced by MOSFETs and Insulated Gate Bipolar Transistors (IGBT). When MOSFETs or IGBTs are used, the capabilities of high voltage pulsed circuit are greatly enhanced, because these devices can be gated off and on. These circuits have the capability to vary the pulse width even on a pulse-to-pulse basis, and the circuits may also be

operated at high repetition rates. Within the limits of their current rating (which can be increased by paralleling devices), these switches give the circuit topologies of very low source impedance, thereby allowing the load to vary over substantial impedance range. As the lifetime of semiconductor devices is substantially high, the expected lifetime of properly designed circuits is also very high. There are two techniques to make the pulses required for this application. The first technique uses resonant pulse compressors to reduce the pulse duration with little loss of pulse energy, combined with linear pulse transformers to increase voltage capabilities. The All Solid State Pulsed Power Supply (ASSPPS) is based on this approach. The second technique more recently reported, involves the reduction in the duration of the pulse, which can be directly switched by a semiconductor switch, through careful conditioning of device turn-on by both snubbers and saturable magnetic assist elements [2].

In this article, we discuss magnetic pulse compression design, material selection and performance of the IGBT based ASSPPS, developed for CVL of 1500 mm long and 47 mm diameter discharge tube. It requires about 1 J pulse energy and operates at 5 to 7 kHz repetition rate. An ASSPPS reported earlier was made with thyristor as the main switching device [3]. In an IGBT, unlike in a thyatron, there is no di/dt limitation due to uniform spread of conduction plasma. The device is self-commutating, and it does not need command charging circuit [4], thereby reducing the overall complexity of the circuit and cost. In certain applications of CVL, it is critical to maintain the timing or jitter of the ASSPPS such that the pulsed output of the laser can be synchronized with another system. The jitter due to the magnetic compression circuit is the result of pulse-to-pulse variations in the total propagation delay that emanates from the fluctuations in the charging voltage of the modulator. In some cases, this synchronization must be held to less than 5 ns. The voltage variation (ripple) causes same variation in propagation delay.

### 2. Magnetic Pulse Compression Details

Fig.T.1.1 shows the electrical circuit of an IGBT based SSPPS which consists of

- A Switch Mode Power Supply (SMPS) [5] (which provides a regulated supply of 350-550 V DC, from  $3\phi$ , 50 Hz, 415 V  $\pm$  15 % mains supply),
- A resonant charging circuit of inductor  $L_0$ , capacitor  $C_0$  and blocking diode  $D_2$ ,
- A pulser section, (which includes a magnetic assist,  $MA_1$  and  $MA_2$ , a pulse transformer T/F of single turn primary and multi-turn secondary (22 T/turn), with two IGBTs as switching device,  $S_1$  and  $S_2$ ), and

- d) A two stage non-linear pulse-forming network named Magnetic Pulse Compression (MPC) circuit, which consists of saturable inductors  $L_1$  and  $L_2$ , and high voltage pulse discharging capacitors  $C_1$ ,  $C_2$ , and  $C_3$ . The output of the MPC is coupled through a pulse cable (RG220) and connected across the laser head and a peaking capacitor  $C_p$ .

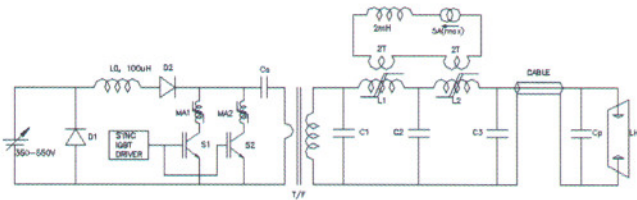


Fig. T.1.1 The IGBT driven two stage ASSPPS.  $C_0=2.2 \mu F$ ;  $C_1, C_2=4nF$ ;  $C_3=1nF$ ;  $C_p=1nF$

## 2.1 Principle of operation and practical considerations

The required power for excitation of the laser is set by the SMPS [5]. The capacitor  $C_0$  resonantly charges to about twice the input DC source voltage through the inductor  $L_0$ , diode  $D_2$  and primary of the pulse transformer. In this circuit, the charging time is about 80  $\mu s$ . After charging of  $C_0$ , in each pulse, the main-switches are turned on for 5  $\mu s$  by ultra-fast gate driver circuit. The main switch consists of two 1.2 kV/400 A IGBTs (in parallel). The magnetic assists  $MA_1$  and  $MA_2$  are placed in series with the IGBTs to help in zero current turn-on by introducing a collector current delay of approximately 500 ns, after the device turns on. This delay is a function of charging voltage of  $C_0$ . These magnetic assists also help, if there is any mismatch in the dynamic characteristics of the switching device, to share equal current while conducting. When the magnetic assist saturates,  $C_0$  discharges through the primary of the pulse transformer and simultaneously charges  $C_1$  to approximately 22 kV through the secondary. While discharging  $C_0$ , the peak current is about 3600 A, half sine wave of 1.2  $\mu s$  width. A low leakage inductance pulse transformer with a step-up turns ratio of 1:22 is used to generate the high voltage to the magnetic pulse compression (MPC) circuit. The volt-second product is sufficient to saturate the core of  $L_1$  (at the end of charging of  $C_1$ ). The charge stored in  $C_1$  then discharges through  $C_2$ . Since the impedance of the discharging path is many times lower, which corresponds to the saturated permeability of inductor  $L_1$ ,  $C_2$  charges faster than  $C_1$ . Similar process continues in  $C_2$  to  $C_3$  also, thereby reducing the rise time of the output pulse. The 1.2  $\mu s$  rise time of the initial voltage pulse on  $C_1$  is compressed to 280 ns in  $C_2$ , and further compressed to <80 ns in  $C_3$ . The maximum voltage as high as 18 kV was

achieved at the output of MPC with a switching input energy approximately of 1 J at an efficiency of 75%. The ASSPPS module typically operates at the initial charging voltage of  $C_0$  at 900 V. The range of operating voltage of the ASSPPS can be varied to adjust the laser output energy.

The flux swing in the pulse transformer is less than 50% of the available volt-seconds product of the core to keep the losses and internal dissipation low. As the resetting of pulse transformer takes place during resonant charging of  $C_0$ , the transformer core does not need a DC reset current circuit. The IGBT collector-emitter voltage falls, on being turned on, the main current is delayed by magnetic assist (MA). The MA provides approximately 0.5  $\mu s$  of hold-off at 1 kV voltage on  $C_0$ . This also reduces the switching losses of the IGBT during turn-on. The supply was tested up to maximum pulse repetition rate of 10 kHz at an input power of 10.5 kW, when capacitor  $C_0$  was charged to ~ 900 V [6]. During the initial (about one-hour) operation of the laser, it offers a non-linear high impedance load. It is therefore not possible to effectively couple the output energy to the discharge tube. This energy reflects from the load, backwards to the input, causing the reverse voltage on the main switching device. The body diode of the device conducts and charges the  $C_0$  in reverse. A resistor-diode (R-D) clipper is included across  $C_0$  to absorb the reflected energy and prevent  $C_0$  from charging with reverse polarity. The saturable inductors of the MPC are made with Ni-Zn based ferrites. The Ni-Zn ferrites were chosen due to their high resistivity ( $\sim 10^9$  ohm-cm) which allows the winding to be in direct contact with the toroids, thereby maintaining high fill-factor and also simplifying the mechanical assembly. Since the available flux density swing is low (0.6 T max), a large volume of the material is required, which gives more surface area for core cooling. The circuit is forced cooled by transformer oil. This transformer oil acts as an insulator and coolant also.

The factors which can influence the magnetic modulator pulse propagation delay include primary switch jitter, voltage regulation of the main source, regulation of the bias power supply for gate driver, regulation of the reset bias source, temperature related effects on magnetic material, capacitors and electronic components etc.[7]. The initial experiments with ASSPPS have identified that the primary cause of the timing jitter is voltage regulation of the main sourcing power supply. The sensitivity of this factor can vary from 3 to 12 ns per volt over operating voltage range of the laser. Increasing the bias current will reduce the jitter, since this will push the core further into negative saturation, where it is less sensitive to bias current regulation, as the core is driven deeper into reverse

saturation. The resetting also helps in reduction of volume required for the inductor  $L_1$  and  $L_2$ . The reset bias current, which is flowing opposite to the main current, keeps the flux density level in the core closed to  $-B_S$ . The reset bias current is applied through an additional winding on each MPC. The reset winding of 2 turns with 30 kV, PTFE wire is magnetically coupled with each stage MPC cores  $L_1$  and  $L_2$ . The reset windings are connected in series with a reset inductor and current source. It is made by a 2 mH air core and a variable DC current source with 5 A (max.). The magnetic excursions of each MPC core are stretched to their negative saturation ( $-B_S$ ) by reset current. Voltage reflections remaining within the ASSPPS after the main pulse generation can also cause jitter in magnetic modulators. Another potential source for jitter is the IGBT switch. A very low jitter high current fast driver was developed to reduce the jitter of the switch. The cause of drift is mainly due to temperature changes in magnetic cores. The variation in temperature can affect the allowable flux swing and therefore saturation time of the core.

### 3. Components and Material Selection.

Selection of components and materials and its critical parameters, which influence the design is discussed in this section.

#### 3.1 Selection of Magnetic cores.

The core selection was based on the critical parameters such as flux density, resistivity of material, power density and core loss at the rated repetition rate, square-ness ratio of B-H loop, availability and cost etc. The low power loss density in Ni-Zn ferrite, combined with good thermal conductivity and monolithic structure (ceramic), allows efficient cooling throughout the volume of quite large cores through conduction from surface, compared to Matglass, which is loosely wound ribbon cores in insulating protective cases. The core loss in amorphous metals is difficult to handle by conduction at high repetition rate because of its poor conduction properties. When a magnetic field is applied in the forward direction, the flux density (B) increases in a somewhat linear fashion initially and then saturates. During initial period, the element appears as highly inductive, where the inductance is proportional to the pulse permeability, and offers high inductive reactance. In saturated region, the derivative of B with respect to H approaches zero and correspondingly, the inductive effect of the material vanishes. The same analysis holds when applied magnetic field is reduced and then reversed in opposite direction. The property of large permeability change in magnetic material is useful for pulse switching applications that resembles a switch. The Ni-Zn ferrite is chosen for

MPC stages, because the maximum flux density of available core is 0.62 T and the resistivity of the core is very high ( $10^7 \Omega \cdot \text{cm}$ ). Therefore, it is possible to place the winding in direct contact with the core (without insulation). This improves the fill-factor of MPC inductor. The development of MPC [7] was initiated with CMD5005 Ni-Zn ferrite cores and later similar grade ferrites have been developed indigenously for this application.

The series magnetic switch introduced as magnetic assist (MA) in the circuit initially offers high impedance in the circuit. This delays the main pulse current. As the core saturates, it offers very low impedance. The selection of core for this MA depends mainly on maximum permeability and available flux swing. The Mn-Zn ferrite is selected as MA, the selected core is T45-20-10 from COSMO ferrites.

#### 3.2 Selection of Switching Device

The selection of the device for this pulser application is based on blocking voltage ratings, peak and forward current, di/dt rating, switching characteristics such as turn-on and turn-off, switching frequency, losses etc. Among the solid state devices analyzed and tested, IGBT was found better suitable at the specified repetition rate due to simple gate control, high blocking voltage, high pulse current carrying capability. Commercially available 1200 V/400 A device was tested and compared with the early designs based on devices such as SCR, GTO and RCT etc. The peak current requirement of this pulser is about 3600 A (pulse duration of 1.2  $\mu\text{s}$  base width, (half sine-wave)), when the capacitor  $C_0$ , charges to  $\sim 900\text{V}$ . The repetition rate is 5 to 10 kHz. Hence two devices of 1200 V/400 A are used in parallel. For parallel operation of devices, their forward and conduction voltage-current characteristic should match in order to share equal current. The device that has more voltage drop will conduct less current and vice-versa. The IGBTs are negative temperature coefficient devices at lower collector current ( $I_C$ ) region, and at high current levels, all type of IGBTs behaves as a device of positive temperature coefficient. Hence the IGBTs are comparatively easy to connect in parallel in the high pulse currents, similar to MOSFETs. In addition, necessary precaution is taken by connecting MA in series with each IGBT, to equalize the pulse current.

#### 3.3 Selection of Capacitors

- Low Voltage (initial storage) Capacitor ( $C_0$ ).

The selection of the capacitor ( $C_0$ ) is based on the following critical parameters, such as low loss tangent, high thermal stability, high pulse current capability, low dielectric absorption etc. Film foil polypropylene with interleaved aluminium foil

conductors fully extended, is one of low loss dielectric material, which has high pulse current capability. This is most suitable for input of the initial storage capacitor,  $C_0$ , in the pulser section. A custom made, bush type fully polypropylene film with extended foil aluminium capacitor of  $0.14 \mu\text{F}/1500 \text{ V}$  (AC RMS) was indigenously developed and bulk fabricated for this purpose. 24 such capacitors were connected in parallel as initial storage capacitor. This capacitor ( $C_0$ ) charges in approximately  $80 \mu\text{s}$  and discharges in  $1.2 \mu\text{s}$ .

b) High voltage side Capacitors.

Strontium titanate ceramic capacitor of  $2 \text{ nF}/40 \text{ kV}$  having very low loss tangent and the above said characteristics, was selected for this application and two such capacitors were connected in parallel, in each stage of the magnetic pulse compressors. The output of the MPC is terminated with a  $2 \text{ nF}/40 \text{ kV}$  peaking capacitor and directly connected on laser head.

4. Construction:

The SSPPS was assembled in two oil-sealed cylindrical chambers. They were connected through a pipe to flow the coolant transformer-oil. The pulser section was placed in first chamber (larger cylinder). The MPC section was placed in second chamber (Smaller cylinder). Transformer oil (as per IS 335) was used as the coolant. All the components were fully immersed in this oil. Both the chambers were tested to be pressure and leak tight. The transformer oil was circulated through these chambers at a flow rate of approximately 5 LPM. The hot oil was taken out of the chambers to be cooled by external cooling tower/ heat exchanger. The temperature at the inlet of coolant must be less than  $45^\circ\text{C}$  for reliable operations.

4.1 Gate Driver circuit

On applying a positive voltage pulse to the gate-emitter terminals, the IGBT is turned on. The gate threshold voltage is approximately 5V. In order to minimize the dynamic loss at turn on, the switching turn-on time must be as short as possible. The speed of the insulated gate type device is related to the rate of supply of charge to the gate input capacitance [8] and gate drive current. This is true for IGBTs also, except during the falling edge of the collector current. This requires the effective gate emitter capacitance (including the Miller effect) to be charged rapidly by a current pulse supplied by a low impedance drive circuit. The dynamic behaviour of the IGBT is affected by unavoidable parasitic capacitance of the structure, often referred to gate to emitter capacitance ( $C_{ge}$ ), collector to emitter capacitance

( $C_{ce}$ ), and collector to gate capacitance ( $C_{cg}$ ). Such parasitic capacitance, together with stray inductance, gate bias current, and driving impedance define the device turn-on performance in terms of switching speed and power loss. During turn-on, the power loss is mainly dependent on the rate of change of collector current ( $di_c/dt$ ) and the dynamic saturation voltage phenomenon.

When the IGBT gate driver output is high, it gives +15 V to the gate and when it is off, the output is -5 V. This negative bias improves the noise immunity and also makes sure that the IGBTs are in OFF state in high noise environment. This driver is capable of sourcing and sinking a peak current of 20 A during ON and OFF switching transitions.

4.2 Pulser Section

$L_0$  is an air core resonant charging inductor placed as shown in Fig.T.1.2. Two IGBTs of  $1200 \text{ V}/400 \text{ A}$  were used in parallel as the main switching device. The IGBTs were mounted on a oil-cooled heat sink shown in Fig.T.1.3.  $C_0$  is a combination of 24 polypropylene film, cylindrical, stud type capacitors connected in parallel and mounted directly on the primary winding of pulse transformer, as shown in Fig.T.1.4. R-C snubber is connected across each device for priming and to reduce the  $dv/dt$ . Separate saturable inductors are employed as MA for each IGBT, which helps in sharing the current and also to reduce the turn-on loss by switching device in zero current switching (ZCS) transition. The MA is constructed using Mn-Zn toroidal core T45-20-10 with 18 SWG triple insulated magnet wire, two strands in parallel having 20 turns. 24 such MA inductors were connected in parallel to carry the current.

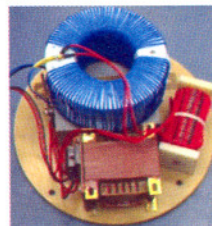


Fig.T.1.2: Input filter and charging inductor



Fig.T.1.3: An assembly of Top Flange of pulser section



Fig.T.1.4: Pulse transformer and capacitor  $C_0$



Fig.T.1.5: A view of IGBT mounting on heatsink

The IGBTs were mounted on an aluminium heat sink as shown in Fig.T.1.5. This was cooled directly by transformer oil, which directly entered into the cavity provided in the heat sink and after cooling the device, the oil flows inside the oil chamber. The heatsink was mounted on top flange of the pulser section of the oil chamber. The following components such as IGBTs, heatsink, signal terminal, input and output terminals and blocking diodes were mounted directly on the top flange of pulser section chamber as shown in Fig.T.1.5. The pulse transformer having turns ratio of 1:22 was developed using Ni-Zn ferrite toroids (154 mm OD, 100 mm ID, 15mm height). Six such ferrites were stacked and high voltage secondary was wound on it as shown in Fig.T.1.6. The secondary had 22 turns. A high voltage wire (of 30 kV PTFE insulation), with silver coated copper conductor (39 strands/28 SWG) was used to make the secondary windings. The primary of this pulse transformer had only one turn. Cylindrical shaped, silver coated copper housing was made as single turn primary. The stacked cores and secondary were placed inside the cylindrical primary as shown in Fig.T.1.6. The snubber components were mounted on an aluminium plate as shown in Fig.T.1.7. 1800 V/200A capsule diode, 10  $\Omega$ /25 W aluminium housed non inductive resistors (in series-parallel combination) were connected to absorb the reflected energy from load side, in case of mismatched load. It is observed that during the initial period of operation of laser, part of energy is reflected back as the laser head impedance is high (mismatched impedance). The complete assembly of pulser side components is shown in detail in Fig.T.1.8.



Fig.T.1.6: Pulse transformer core and secondary winding

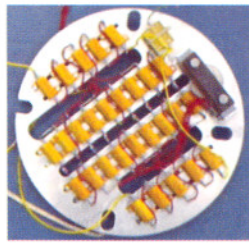


Fig.T.1.7: Diode - Res. Clamping and snubber Circuit assembly.

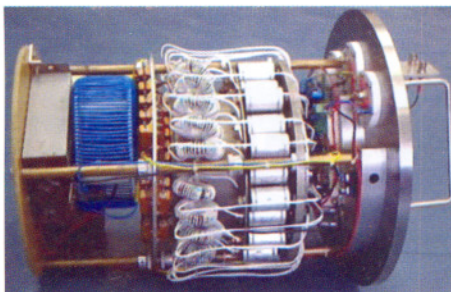


Fig.T.1.8: Assembly of pulser section.

### 4.3 Magnetic Pulse Compression Section

CMD 5005 Ni-Zn ferrite cores (3 Nos. each) are used in both  $L_1$  and  $L_2$  as saturable inductors. The cores were toroidal in shape with a dimension of 154 mm O.D, 100 mm I.D and 15 mm height.

The MPC toroids were held together with 8 mm (dia) brass rods and specially made FR4 grade PCB of 6 mm thick and 105  $\mu$ m thick copper tracks, where the PCB provides necessary holding and support to ferrite toroids, which makes the required number of turns of the winding, with this arrangement the fill factor will improve drastically and approaching towards 1. There were 4 parallel paths in  $L_2$  inductor, which were evenly distributed over the periphery of the winding. The saturable inductors  $L_1$  and  $L_2$ , capacitors  $C_1$  and  $C_2$  and their assembly is shown in Fig.T.1.9. The reset winding (two turns each) for  $L_1$  and  $L_2$  made by 30 kV PTFE insulated silver coated, 39/28 copper wire and were connected in series with a 2 mH air core inductor as discussed in section 2.1. The input and output terminations of the MPC section were made through PTFE high voltage insulators. These insulators were fixed at the top of flange of each chamber.

### 5. Protection:

The following protections are incorporated in the ASSPPS

- 1) Over temperature protection for device: When the temperature of the heat sink of device exceeds about 55°C, the thermal switch operates, and disables the gate drive auxiliary power supply of the device and stops triggering.

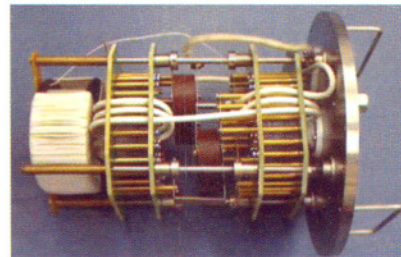


Fig.T.1.9: Assembly of Magnetic Pulse Compression section.

- 2) During the initial period of the operation of laser, there is mismatch in laser load impedance and modulator output impedance, which induces reflections of unused energy. This is destructive to the device. A Resistance-Diode clamp circuit is placed across the  $C_0$  to absorb the reflected energy and dissipate it in resistance, thereby reducing the effect of the reflections in the device.

6. Results

The prototype of the SSPPS was tested extensively to check its performance. Some of the key waveforms of solid-state pulser are given here. Two switching devices were used in parallel, in SSPPS as main switching device.

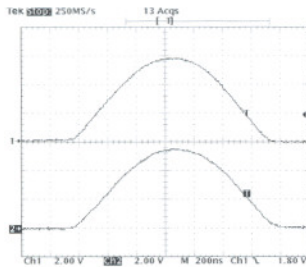


Fig.T.1.10: Current in each IGBT (600 A/div)

Fig.T.1.10 shows the current of each device. The current through the devices are sharing very closely. Similar test was carried out using two different make devices, having same ratings, shows the sharing of equal current. This result was taken at  $C_0$  capacitor voltage 800 V and repetition rate of 10 kHz. Fig.T.1.11 shows the switching voltage (Ch-3), current of a device (Ch-2), and charging voltage of  $C_1$  capacitor (Ch-4). The switching current is the current through one device. The actual current through the primary of pulse transformer is twice that of device current. From Fig. T.1.11 it is concluded that the device current reaches zero, when the  $C_1$  voltage reaches its maximum.

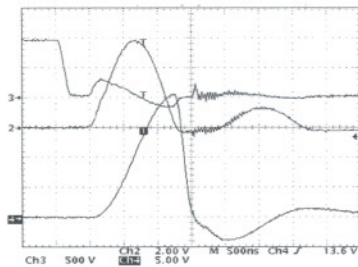


Fig. T.1.11: Trace3: IGBT voltage 500 V/div, Trace2: a IGBT current 600 A/div, trace4: C1 voltage 5 kV/div

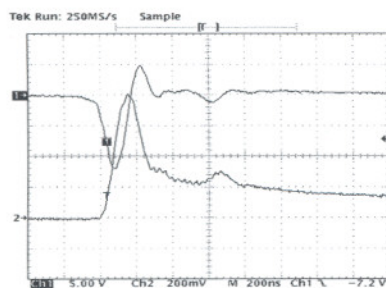


Fig. T.1.12: Trace1 laser head vol. 5 kV/div, Trace2 its current not in scale

Later, as the inductor  $L_1$  saturates, it transfers charge to next stage (discharging of  $C_1$  and charging of  $C_2$ ) faster than its charging time. Fig.T.1.12 shows the output voltage across laser head (Ch-1) and its current shape (Ch-2). The voltage rise time is less than 80 ns at 13 kV peak. The current shown is not in scale due to the geometrical limitations in monitoring it. The observations were recorded when the tube temperature was at about 1500° C. Fig.T.1.13 shows the laser wave shape monitored through biplaner vacuum photo diode with plane-plane (100% and 4%) mirror arrangement.

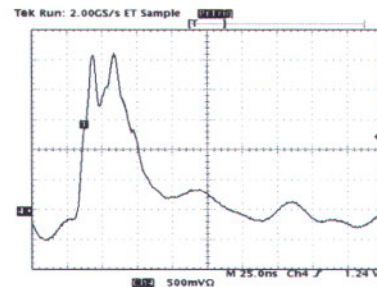


Fig.T.1.13: Laser pulse shape

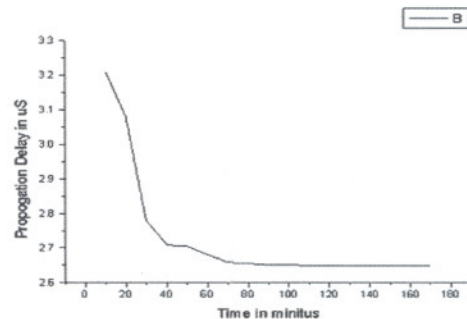


Fig.T.1.14:Drift versus time curve

The solid-state pulser and laser start from cold condition. The magnetic components and the coolant take time to stabilize. This change in temperature introduces a change in delay from external trigger to laser output pulse called drift. Fig.T.1.14 shows the output drift measured with respect to time. Fig.T.1.15 shows the output jitter of laser pulse at about 6 kHz repetition rate [9]. The total jitter is  $\pm 2.5$  ns. Fig.T.1.16 shows the photo of cylindrical prototype of pulser and magnetic pulse compression stages. The complete solid state pulsed power supply along with switch mode power supply is shown in Fig.T.1.17. The suitability of this system was checked by connecting it to the CVL laser load. The system performed satisfactorily and maximum power of 33 W was achieved. The reliability of the system was checked by operating the system continuously for 100 hours, and heat accelerated test with laser load, under normal operating conditions was carried

out. During 100 hours continuous run, it was observed that, as the time elapsed, the optical power output reduced, as the copper density reduced in the plasma tube of laser. Other output parameters of the system were normal.

During heat accelerated test, the temperature of the transformer oil of the system was elevated from 45°C to 80°C, by shutting off the cooling and maintaining the coolant temperature at 80°C. The system was operated for 5 hours continuously. This heat-accelerated test proved that the system reliability is better than that of conventional thyatron based pulsed modulators.

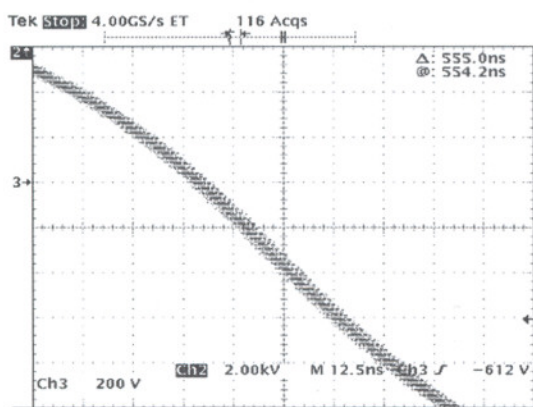


Fig. T.1.15: Output Pulse jitter of ASSPPS



Fig. T.1.16: Photo of first cylindrical proto type of pulser and magnetic pulse compression stages

**7. Conclusion:**

An All Solid State Pulse Power Supply is developed and tested to suite the stringent conditions of single CVL and MOPA chain applications. The ASSPPS was tested at a variable repetition rate from 5 kHz to 10 kHz with 47 mm dia, 1500 mm long copper vapour lasers. The results were compared with the thyatron based conventional pulse power supplies operating at a repetition



Fig.T.1.17: All Solid State Pulsed Power Supply

rate of 5 kHz to 7 kHz with similar laser load. It is observed that the results are highly comparable. Therefore, the developed ASSPPS can replace the existing thyatron based pulsed power supplies for CVLs of similar characteristics. The use of the ASSPPS significantly improves the operation cost of running of CVLs

**References :**

1. M. Nehmadi, Z. Kramer, Y. Ifrah, and E. Miron, J.Phys. D, Appl.Phys.**22**, 29 (1989).
2. J.Vitins, J.L. Steiner, A. Schweizer and H. Lawatsch, IEEE Conference Record of Eighteenth Power Modulator Symposium, 229 (1988).
3. Dharmraj V Ghodke, K.Muralikrishnan, R.Bhatnagar, Proceedings of DAE BRNS National Laser Symposium, 85 (2001).
4. D.Chatroux and J.Maury, Proc. SPIE Vol.1859, Laser Isotope Separation (1993).
5. Dharmraj V Ghodke and Muralikrishnan. K, Proc. DAE BRNS National Laser Symposium NLS-2 (2002)
6. Dharmraj V Ghodke and Muralikrishnan. K, Proc. DAE BRNS National Laser Symposium NLS-2 (2002).
7. H.J. Baker, P.A.Ellsmore and E.C Sille, J.Phys.E:Sci.Instrum. **21**, 218 (1988).
8. M.Melito and F.Portuese, Proc. Power Conversion on Intell. Motion, 153 (1990).
9. Dharmraj V Ghodke, K.Muralikrishnan and U.Nundy, Proc. DAE-BRNS National laser Symposium NLS-4 (2005).